JURNAL KIMIA VALENSI
p-ISSN: 2460-6065; e-ISSN: 2548-3013
Journal homepage: https://journal.uinjkt.ac.id/index.php/valensi
Research Article

Development of a Low-Cost Reflectance Visible Spectrophotometer with Chemometrics for *Curcuma xanthorrhiza* Roxb. Quality Control

Rudi Heryanto[1,2], Dyah Iswantini[1,2*], Eti Rohaeti[1,2], Mohamad Rafi[1,2], Novia Rahma[1], Nurul Hafshah[1], Eni Mardiana[1]

[1]*Department of Chemistry, Faculty of Mathematics and Sciences, IPB University, Bogor, 16680, Indonesia*
[2]*Tropical Biopharmaca Research Center, Institute for Research and Community Service, IPB University, Bogor, 16680, Indonesia*

[*]*Email: dyahis@apps.ipb.ac.id*

Article Info
Received: July 18, 2024
Revised: July 18, 2024
Accepted: Oct 3, 2024
Online: Nov 30, 2024

Citation:
Heryanto, R., Iswantini, D., Rohaeti, E., Rafi, M., Rahma, N., Hafshah, N., & Mardiana, E. (2024). Development of a Low-Cost Reflectance Visible Spectrophotometer with Chemometrics for *Curcuma xanthorrhiza* Roxb. Quality Control. *Jurnal Kimia Valensi*, 10(2), 192-204.

Doi: 10.15408/jkv.v10i2.40351

Abstract

A simple, portable visible reflectance spectrophotometer was developed for classifying the quality of *Curcuma xanthorrhiza* Roxb. The device was assembled using consumer electronic components: an LED as the light source, a DVD optical layer as the diffraction grating, and a webcam as the detector, with web-based software (Spectral Workbench) as the signal processor. The spectrophotometer's performance was evaluated using standard Sudan III samples and powdered *C. xanthorrhiza* samples from two quality classes (A and B). Spectral data were analysed using principal component analysis (PCA) and partial least squares (PLS) regression. PCA successfully grouped Sudan III samples by concentration and classified *C. xanthorrhiza* by curcuminoid content. A PLS regression model was developed for quantifying Sudan III, yielding R^2 values of 0.9909 for both calibration and cross-validation, with RMSEs of 0.3821% and 0.4152%, respectively. The results closely matched those from a commercial spectrophotometer. A PLS-discriminant analysis (PLS-DA) classification model for *C. xanthorrhiza* was also developed, achieving sensitivity and specificity values of 1. Additionally, semi-quantitative parameters such as decision limit (26.15% B), detection capability (41.06% B), and unreliability range (26.15–41.06% B) were calculated. The classification model showed strong sensitivity, specificity, and detection capabilities within acceptable limits. These findings suggest that this low-cost reflectance spectrophotometer, combined with chemometric methods, holds promise as a practical tool for the quality control of raw herbal materials.

Keywords: Chemometrics, *Curcuma xanthorrhiza* Roxb., Reflectance Spectrophotometer, Herbal Quality Control

1. INTRODUCTION

In Indonesia, medicinal plants, either alone or mixed with others, can be made into herbal products in the form of jamu, standardized herbal medicines, and phytopharmaca [1]. Despite the long history of using herbal products in Indonesia, there are several aspects of the herbal product supply chain that remain underdeveloped. For instance, farmers, who are the main suppliers of raw materials for medicinal plants, typically sell these materials without conducting any quality sorting. Consequently, they are paid based solely on the weight of the raw materials, regardless of quality. This results in farmers receiving only a small portion of the economic value compared to the price paid by final consumers of herbal medicines [2]. Introducing methods for analysing the quality of raw materials to medicinal plant farmers could help address the unequal distribution of profits within the herbal product supply chain.

Current quality control methods for raw materials and herbal products often rely on chromatographic or spectroscopic techniques [3]. High-performance liquid chromatography (HPLC), gas chromatography (GC), and thin layer chromatography (TLC) are the primary chromatographic methods used for quality analysis of natural materials [4]. These techniques produce a fingerprint chromatogram that

displays all the unique chemical compounds in the raw material or herbal product. While highly accurate, these methods require significant time and sample preparation [5]. Another approach to assessing the quality of raw materials and herbal products is spectroscopy [6]. Spectroscopy works by detecting changes in the chemical composition of a material, which can alter its optical properties, such as absorbance, transmission, and reflection [7]. Several studies have demonstrated the use of spectroscopic methods for quality control of medicinal plants based on their active compound composition [8]. The most commonly used spectroscopic technique is Fourier transform infrared spectrophotometry (FTIR) [9]. However, other methods, such as UV-Vis spectrophotometry, are also effective for this purpose[10].

The quality control methods mentioned above are analytical techniques developed in a chemical laboratory setting, making them difficult for farmers, who supply herbal raw materials, to access directly. It would be highly beneficial for farmers if there were alternative methods that were simpler and more cost-effective for quality control of raw materials. One such alternative is the development of a portable reflectance spectrophotometer, an analytical instrument that provides straightforward results to the operator when brought to the sample, essentially allowing the spectrophotometer to go to the sample rather than the sample to the spectrophotometer [11]. Reflectance spectrophotometers also offer practicality in measurements by enabling direct measurement of solid samples [12]. Furthermore, these spectrophotometers can be developed using consumer electronic components. Essentially, a spectrophotometer can be assembled from components such as a white LED light source, a DVD for the dispersing medium, a CCD/CMOS webcam as the detector, and image-based data acquisition/processing software or a direct spectrum recorder [13]. A low-cost multifunctional webcam spectrophotometer has been developed and applied to perform molecular absorption and fluorometric measurements, with results comparable to those obtained from commercial spectrophotometers [14]. Additionally, a spectrophotometer with LED light source components and a webcam detector has been created, capable of producing representative fluorescence spectra from various fruits such as apples, cherries, and pears [15].

Raw materials and herbal products are complex chemical systems. Quality control methods based on pattern recognition, such as spectroscopic fingerprinting or chromatography, can be effective in exploring the complexity of these phytochemicals [16]. Fingerprint data, being inherently complex, cannot be easily evaluated. The similarities or differences in patterns within sample fingerprint data can only be revealed using appropriate chemometric methods. Commonly used chemometric methods for this purpose include multivariate techniques for data exploration, classification, or calibration, such as Principal Component Analysis (PCA) and Partial Least Squares-Discriminant Analysis (e.g., PLS-DA)[17]. The combination of UV-Vis reflectance spectroscopy and chemometrics has been successfully employed to differentiate Angelicae sinensis simplicia roots from four similar herbs [18] and to identify adulteration in ginseng [19].

This research aims to develop a portable visible reflectance spectrophotometer for quality control of herbal raw materials using consumer electronic components. For portable systems utilizing consumer electronics, device-to-device performance repeatability can be a challenge [20]. Additionally, any developed portable spectrometer must produce results with verifiable analytical performance [21]. As a first step in developing a quality control system based on a reflectance spectrophotometer, this paper presents the configuration of the constructed reflectance spectrophotometer and demonstrates its performance using a Sudan III standard compound. The results are compared with those obtained from a commercial spectrophotometer. Subsequently, the reflectance spectrophotometer and chemometrics were applied to classify *Curcuma xanthorrhiza* Roxb. of different quality, based on the composition of the main chemical components, curcuminoids. *C. xanthorriza* is a widely recognized medicinal plant used in various herbal remedies (*Jamu*). Pharmacological studies have demonstrated its anti-inflammatory, antibacterial, antioxidant, neuroprotective, nephroprotective, antitumor, and hepatoprotective properties, attributed to its xanthorrhizol and curcuminoid content[22,23]. The obtained classification model is evaluated by calculating key quality parameters (sensitivity, specificity) [24] and three additional semi-quantitative parameters (decision limit, detection ability, and unreliability region) [25].

2. RESEARCH METHODS

2.1 Sample

Two types of samples were used in this research. The first sample is the Sudan III standard sample (Merck). Standard Sudan III was used to test the analytical performance of the reflectance spectrophotometer against commercial spectrophotometers. The second sample was powdered raw materials of *Curcuma xanthorrhiza* Roxb. The sample was originated from *C. xanthorriza* cultivated in the Biophamaca field station of TROPBRC IPB, Bogor, Indonesia. It was harvested and processed following the established procedures at the facility. Two different powdered sample used in this research. Powdered raw material of *C.*

xanthorrhiza A is made from fresh rhizome and has higher curcuminoid levels than raw material B, which has a shelf life of 2 years **(S1)**. This second sample is used as a case study for the application of reflectance spectrophotometers in the quality control of herbal raw materials. Sudan III samples for measurements using a reflectance spectrophotometer were made in pellet form with a $BaSO_4$ (Merck) matrix **(S2)**. $BaSO_4$ is a standard commonly used as a blank in reflectance measurement mode because it has a reflectivity above 90% [26].

2.2 Development of the Reflectance Spectrophotometer

The reflectance spectrophotometer was constructed based on the scheme in **Figure 1**(i). A white LED flashlight, powered by a transformer with a voltage of 7.4 V, was used as the light source. The positions of the light source, sample holder, grating, and webcam were adjusted so that the angle of incidence of the light was the same as the angle of reflection, specifically 45°. This angle is above the critical angle of the borosilicate crystal used, allowing measurement in ATR (attenuated total reflectance) mode. In the ATR system, the light that interacts with the sample beneath the crystal and the reflected light detected by the detector first passes through a medium with a high refractive index. In this research, the medium used was a glass crystal preparation made from borosilicate, which is transparent to visible light. An optical layer from a DVD was used as a diffraction grating, and a webcam was used as a detector. The spectrum data acquisition process was carried out using Spectral Workbench, a web tool with features for capturing spectra with a webcam, as well as for visualizing, manipulating, and saving spectra from web browser pages [27]. **Figure 1**(ii) shows the constructed spectrophotometer with all its components.

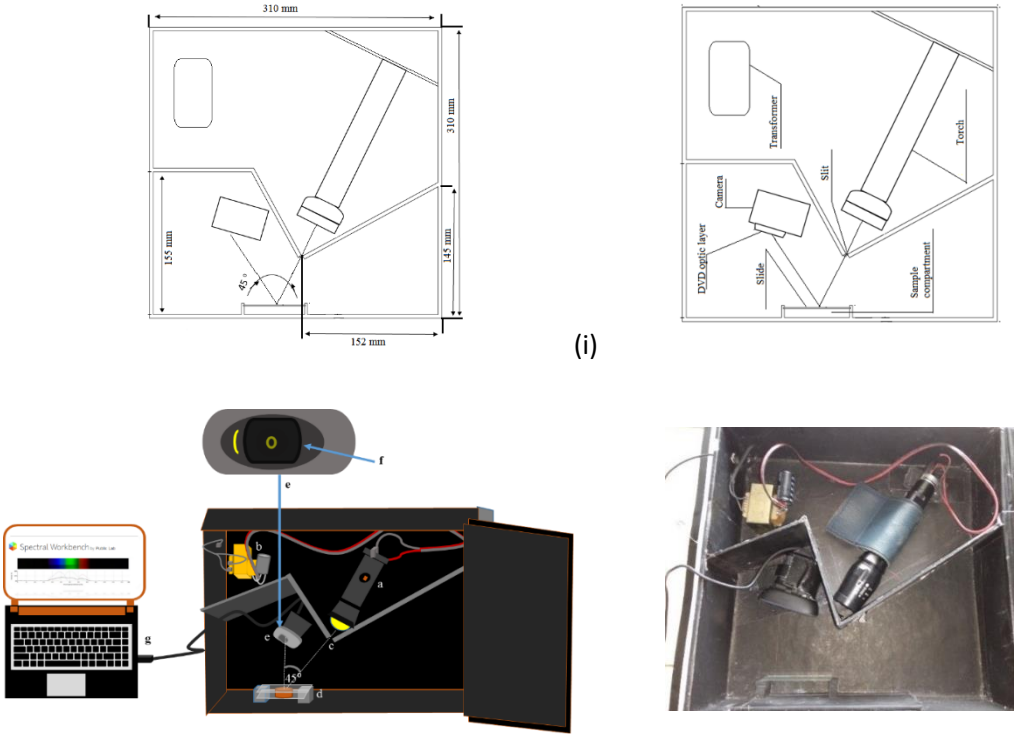

Figure 1. (i) Diagram and (ii) real schematic of the reflectance spectrophotometer: (a) LED light source; (b) transformer; (c) slit; (d) sample compartment; (e) detector; (f) grating; and (g) laptop equipped with the Spectral Workbench application.

2.3 Calibration and Measurement Modes of the Reflectance Spectrophotometer

The reflectance spectrophotometer produces a sample spectrum with the help of tools from Spectral Workbench. When the white LED flashlight is turned on, the light passes through the gap and is directed at the borosilicate crystal at a 45° angle. Light at this incident angle causes internal reflectance and forms evanescent waves (electromagnetic waves that only exist within a very short distance from the boundary or interface between two materials with different refractive indices). These evanescent waves penetrate and interact with the sample, which is in pellet form and placed directly under the crystal. The attenuated evanescent waves are then passed back into the light beam, exiting the tip of the crystal and continuing towards the grating. The grating, attached to the front of the webcam, diffracts the white light into its color

components, which are captured by the webcam sensor. The color spectrum resulting from the grating diffraction is visualized in real time in Spectral Workbench (**Figure 2**). Spectral Workbench simultaneously displays the spectrum with the y-axis representing percent intensity (%I) and the x-axis representing wavelength. To obtain the correct wavelength scale in the spectrum, calibration is first carried out using a CFL light source. Spectral Workbench performs the calibration process by adjusting the spectrum wavelength scale based on the specified CFL emission peaks, namely emission peaks of 436 and 546 nm.

Spectral Workbench acquires sample spectra by converting color spectrum images into data. The resulting data can be exported into XLS format as tabulated wavelengths and intensities, represented by average RGB (I) values. The percent intensity on the y-axis in the transmission spectrum is calculated using the following equation (1):

$$\%\mathrm{I} = \frac{\mathrm{I}}{257}\, x\, 100\% \qquad (1)$$

The reflectance spectrophotometer constructed is a single beam type spectrophotometer. To obtain the reflectance (R) value of the sample, a comparison is made between the intensity of the $BaSO_4$ blank and the intensity of the standard or sample, following the calculations with the equation provided (2) [28]:

$$\mathrm{R} = \frac{\%\mathrm{I}_{Sample}}{\%I_{blank}};\ \mathrm{A} = -\log R;$$

$$\mathrm{A} = \log\frac{1}{R};\ \mathrm{A} = \ log\ \frac{\%\mathrm{I}_{blank}}{\%I_{sample}} \qquad (2)$$

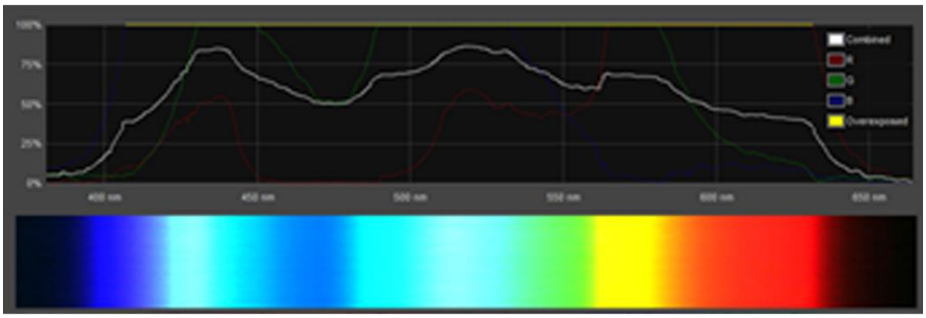

(a)

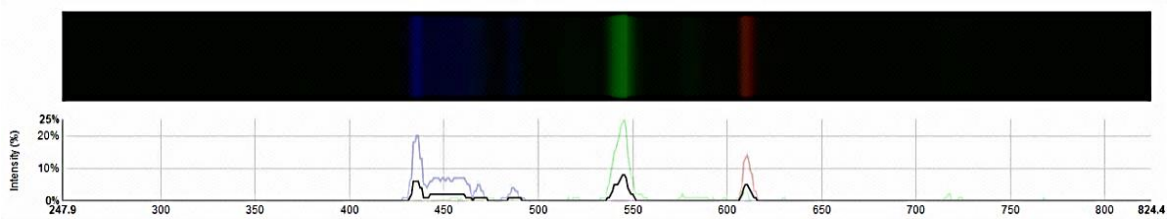

(b)

Figure 2. Example of (a) intensity and color spectrum of $BaSO_4$ blank and (b) wavelength calibration using a CFL spectrum.

2.4 Demonstrating the Performance of the Reflectance Spectrophotometer and Comparing It with Commercial Spectrophotometers

The reflectance spectrophotometer system was developed due to its advantages of speed, non-destructive measurements, and the ability to measure solid samples directly. These benefits arise from the interpretation of the spectrum using chemometric techniques, which can extract analyte information from the background spectrum caused by the sample matrix [29]. The performance of the reflectance spectrophotometer is evaluated by its ability to quantify the amount of Sudan III in the standard pellet. The results were then compared with those obtained from a commercial spectrophotometer.

The quantification of Sudan III in standard pellet samples was performed using a multivariate calibration model. To develop this model, a series of pellets with different concentrations of Sudan III were prepared. The pellets consisted of Sudan III and a $BaSO_4$ matrix, with concentrations of 1, 3, 5, 7, 9, 11, and 13% (w/w). Each concentration was prepared in triplicate. The reflectance spectrum of all standard pellets was measured using a reflectance spectrophotometer. The multivariate calibration model was then constructed from the reflectance spectrum data and the corresponding concentration values.

The commercial equipment used for comparison is a transmission/absorption type UV-Vis Spectrophotometer (Shimadzu UV-1800). Quantification of Sudan III with this

spectrophotometer was performed using a calibration curve. A calibration curve was prepared using a series of Sudan III standard solutions in methanol with concentrations of 5.7, 9, 11, 13, and 15 µg/mL. The absorption of each standard solution was measured at the maximum wavelength (504.5 nm). The standard data were used to create the calibration curve using a univariate linear regression approach.

For the performance tests, standard pellet samples were prepared by mixing Sudan III standard and $BaSO_4$ to a total of approximately 10 g, with a Sudan III concentration of 0.001% (w/w) **(S3)**. The mixture was replicated three times. Each mixture was homogenized and used to create pellets (approximately 500 mg each). The reflectance of these five pellets was measured using a reflectance spectrophotometer, and the concentration of Sudan III was calculated using the developed multivariate calibration model.

To quantify Sudan III using the commercial equipment, the pellets were returned to the original mixture and homogenized again. The mixture was then dissolved in methanol in a 10 mL volumetric flask and diluted 10-fold. The absorbance of each diluted solution was measured five times. Due to the different measurement modes of the two instruments used, the analysis results were expressed as the absolute mass of Sudan III in the mixture. The significance of the analysis results obtained from the two instruments was evaluated using analysis of variance (ANOVA).

2.5 Application of Reflectance Spectrophotometer for Classification of *C. xanthorrhiza* Roxb. Raw Materials

To demonstrate the reflectance spectrophotometer's capability in quality control of raw materials/herbal products, it was utilized to classify *C. xanthorrhiza* samples of varying qualities, specifically *C. xanthorrhiza* A with higher curcuminoid levels compared to *C. xanthorrhiza* B samples **(S1)**. Both samples were in powder form, sized 40-60 mesh, and dried in an oven at 60°C until the moisture content was less than 10%.

The initial step in developing a reflectance spectrophotometer-based classification method involved preparing a set of samples. The reflectance data from these samples was used to construct a classification model (training set) and another set of samples for validating the model (test set). In this study, 65 pellets (each approximately 500 mg) were prepared from both *C. xanthorrhiza* A and B as training samples, along with 25 pellets each for test samples. All samples were measured using a reflectance spectrophotometer to collect spectrum data. Subsequently, a chemometric approach was employed to develop a classification model capable of distinguishing between the qualities of *C. xanthorrhiza* A and B based on the obtained spectrum data.

The quality of classification models is assessed using performance parameters such as sensitivity and specificity [24]. Sensitivity measures the proportion of samples belonging to a class that are correctly identified as belonging to that class. Specificity measures the proportion of samples not belonging to a class that are correctly identified as not belonging to that class. These parameters are calculated based on four possible predictions made by the model: true positive (TP), false positive (FP), true negative (TN), and false negative (FN). TP (True Positive): Number of positive samples correctly identified as positive. FN (False Negative): Number of positive samples incorrectly classified as negative. FP (False Positive): Number of negative samples incorrectly identified as positive. TN (True Negative): Number of negative samples correctly identified as negative. Sensitivity and specificity are calculated using the following formulas (3&4):

$$Sensitivity = 100 \times \left[\frac{TP}{(TP+FN)}\right] \quad (3)$$

$$Spesificity = 100 \times \left[\frac{TN}{(TN+FP)}\right] \quad (4)$$

Additionally, the quality of the reflectance spectrophotometer-based classification model is evaluated using quantitative connotation parameters such as the unreliability region, decision limit, and detection capability [30]. These parameters are determined using the Performance Characteristic Curve (PCC) methodology [25]. In this assessment, it is assumed that high-quality *C. xanthorrhiza* A samples are adulterated with lower-quality *C. xanthorrhiza* B samples.

PCC curves are constructed by predicting samples at various adulterant concentrations using the classification model. Pellets containing *C. xanthorrhiza* B as an adulterant were prepared at concentrations of 10, 20, 25, 30, 35, 40, 50, 60, 70, 80, and 90% (w/w). Each concentration was replicated ten times, resulting in a total of 110 pellet samples. The number of predicted samples classified as adulterated (positive output) or not (negative output) at each concentration was calculated as the predicted fraction, denoted as p(x). The p(x) values were plotted against the concentration of adulterant B. Experimental data points were then fitted to a sigmoid equation (5) using Auto2fit curve-fitting software (CPX Software), as described by López et al. [25], to derive the three model performance parameters.

$$p(x) = \frac{1}{1+ e^{b(x-a)}} \quad (5)$$

2.6 Multivariate Data Analysis - Chemometrics

The reflectance spectrum data was analysed using The Unscrambler X software (Camo Inc.).

Initially, the spectrum data was prepared in MS Excel and subsequently imported into Unscrambler. Before further analysis, the spectrum data underwent pre-processing with the Savitsky-Golay smoothing method. Next, both the spectra of Sudan III and *C. xanthorrhiza* samples were subjected to principal component analysis (PCA). PCA was utilized to assess the suitability of the samples for training calibration and classification models (Springer, 2019).

The correlation between the reflectance spectrum of Sudan III and its concentrations in standard samples was investigated using partial least squares regression (PLSR). This approach facilitated the construction of a multivariate quantitative calibration model, which was employed to evaluate the quantitative performance of the reflectance spectrophotometer in comparison with commercial spectrophotometers.

For classification purposes, the partial least squares-discriminant analysis (PLS-DA) method was applied to develop a model for distinguishing between *C. xanthorrhiza* samples (*C. xanthorrhiza* A and B). PLS-DA correlates the spectrum data of *C. xanthorrhiza* samples A and B with categorical class data, where a value of 1 designates samples in the discriminated class (curcuma sample A) and 0 for samples in the other class (curcuma sample B). The effectiveness of the calibration and classification models was assessed based on the coefficient of determination (R^2) for calibration and cross-validation, as well as the root mean square error of calibration (RMSEC) and root mean square error of prediction (cross-validation) (RMSEP(CV)).

3. RESULTS AND DISCUSSION

3.1 Reflectance Spectrum of Standard Sudan III Samples and *C. xanthorrhiza* Roxb. Samples

This research develops a reflectance spectrophotometer with an ATR measurement configuration, which offers easy and direct measurement of solid samples. The spectrophotometer detects and measures reflected radiation (R) (Equation 2). The resulting spectrum can be displayed in log(1/R) units, which are dimensionally equivalent to absorbance [28].

Figure 3a shows the spectrum of the Sudan III standard sample. The absorbance spectrum of Sudan III solution is known to have maximum absorption at wavelengths of 340-360 nm and 490-510 nm [31]. The Sudan III standard pellet sample shows at least two prominent absorption peaks at 423 and 540 nm. This absorption peak shift from the solution's absorption peak was also observed by Taunaumang et al.[32]. The maximum absorption of Sudan III measured in crystalline solid form shifts to a greater wavelength than that of the Sudan III solution. Differences in measurement configuration from transmission to ATR can cause distortion. One of the distortions introduced by ATR is a shift in the absorption band to lower frequencies (larger wavelengths) [33].

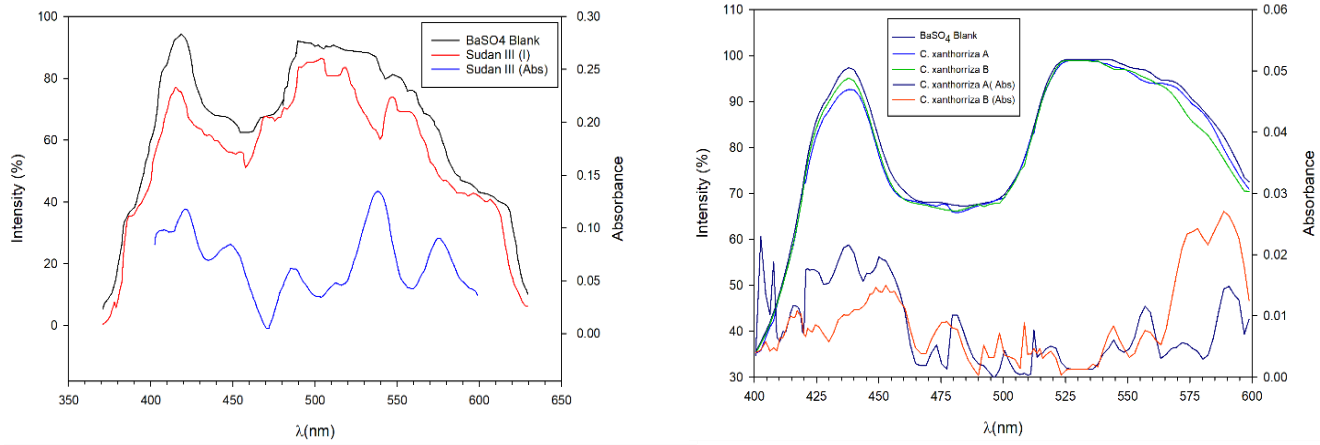

(a) (b)

Figure 3. Sample spectrum with intensity scale from measurements using the reflectance spectrophotometer for the blank/sample and the absorbance spectrum calculated using equation 2: (a) Sudan III and (b) *C. xanthorriza*.

Figure 3b shows the spectrum of *C. xanthorrhiza*. The spectrum of *C. xanthorrhiza* powder results from the overlapping absorption of its constituent components. Among the observable absorption peaks is one in the range of 410-460 nm, which is thought to originate from the absorption of curcuminoids contained in *C. xanthorrhiza*. Suresh et al. [34] reported that *C. longa* samples measured using a UV-Vis Diffuse Reflectance Spectrophotometer produced a spectrum with a wide absorption peak in the range of 400-500 nm. The absorption is mainly caused by electronic transitions in bonding orbitals, lone pairs, and unfilled non-bonding or anti-bonding orbitals of curcuminoids [35].

3.2 Quantitative Performance of Reflectance Spectrophotometers

The reflectance spectrophotometer constructed in this research is intended for use as a quality control or authentication device. For this purpose, signals from a single wavelength do not provide sufficient information to address most authentication problems. Using the spectral profile of a sample as a fingerprint and interpreting it with chemometric methods can address this need [36]. Reflectance spectrophotometers record signals resulting from the interaction between radiation and chemical components in the sample at many wavelengths. It is necessary to demonstrate that this spectrum signal accurately represents the reflectance/absorption of these analytes. Transmission mode spectrophotometers using consumer electronic components have been shown to provide quantitative signals of analytes equivalent to those of commercial instruments [37].

The analytical performance of the reflectance spectrophotometer was determined using the Sudan III standard sample with a $BaSO_4$ matrix. The resulting spectrum in the 400-600 nm range was pre-processed with the 9-point Savitsky-Golay smoothing technique before being evaluated using PCA and PLS Regression. PCA was used as an exploratory tool to visualize variations in spectrum data caused by differences in concentrations of the Sudan III standard sample. **Figure 4a** displays the score plot of samples with variations in Sudan III concentration from 1% to 13%. The first principal component (PC1) and the second principal component (PC2) together account for 99% of the total variance. The large amount of accumulated variance indicates that the score plot represents almost all the information contained in the sample spectrum. The spectrum produced by the reflectance spectrophotometer contains quantitative information on analytes, which can be seen from a clear grouping tendency along the PC1 axis based on differences in sample concentration. A similar trend was observed in the research by Alomar et al.[38], who used PCA to evaluate the spectrum data of Sudan I samples produced by the Surface Enhanced Raman Scattering spectrometer.

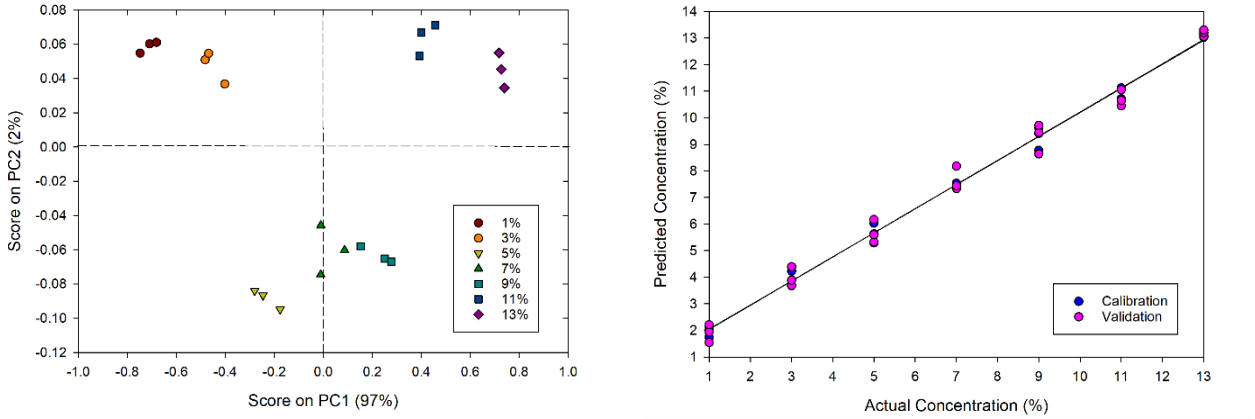

(a) (b)

Figure 4. (a) PCA score plot (PC1 and PC2) and (b) prediction performance of the PLS regression model from the Sudan III standard sample spectrum in the concentration range 1-13%.

The spectrum data used in the PCA model was then reprocessed to create a multivariate calibration model. The PLS regression model was built using Unscrambler X software with the wide kernel PLS algorithm. The performance of the regression model was maintained by cross-validation and optimized using 7 latent variables. **Figure 4b** shows the prediction vs. reference plot for the concentration of Sudan III standard sample. The predicted values in the plot are generated from the PLS regression model, with R^2 values of 0.9909 for both calibration and cross-validation, and RMSE values of 0.3821% and 0.4152% for calibration and cross-validation, respectively. Williams & Antoniszyn [39] explained that a multivariate model with an R^2 value equal to or above 0.99 is considered excellent. The goodness of the calibration model is also supported by the relatively small calibration and cross-validation RMSE values compared to the standard sample concentration values. A model with lower calibration and cross-validation RMSE values, as well as smaller differences between the two, indicates better performance and stability [40]. Another parameter that demonstrates the goodness of the PLS regression model is the RPD (Ratio of Performance to Deviation) value. RPD is a comparison between the reference standard deviation and RMSE. The calibration model has RPD values of 10.7 and 9.9 for calibration and cross-validation, respectively. RPD values above 4.1 indicate a very good model [41].

Table 1. Comparison of Sudan III analysis results from reflectance and commercial spectrophotometers, with ANOVA data evaluation

Sample	Nominal Mass of Sudan III in 10 g of Mixture (g)	Results from Reflectance Spectrophotometer (g)	Results from Shimadzu UV-1800 (g)
Mixture 1	0.0011	0.0012	0.0013
Mixture 2	0.0010	0.0010	0.0011
Mixture 3	0.0010	0.0010	0.0011
Average ± SD	$(1.0\pm0.1)10^{-3}$	$(1.1\pm0.1)10^{-3}$	$(1.1\pm0.1)10^{-3}$

Analysis of Variance (ANOVA)

Source of Variation	SS	df	MS	F count	P-value	F crit
Between Groups	2.89×10^{-08}	2	1.44×10^{-08}	1.444444	0.3075469	5.143253
Within Groups	6×10^{-08}	6	1×10^{-08}			
Total	8.89×10^{-08}	8				

The calibration model was used to determine the amount of Sudan III standard in a new, intentionally created sample. These samples were also analysed using a commercial spectrophotometer in transmission measurement mode. Due to differences in measurement modes, the comparison of sample analysis results is based on the nominal mass of Sudan III. **Table 1** displays the analysis results from both instruments, along with the ANOVA results for the overall comparison of the data. Both instruments produced the same average analysis value. The ANOVA results showed no significant differences in the nominal mass data for Sudan III ($F_{count} = 1.4444 < F_{table}$, 0.05; 2.9 = 5.143253, p = 0.3075469). Therefore, chemometric evaluation and comparison with commercial equipment indicate that the reflectance spectrophotometer can produce signals that accurately represent the analytes in the sample.

3.3 Case Study: Using a Reflectance Spectrophotometer for Quality Classification of *C. xanthorriza* Roxb. Samples

A case study was conducted to explore the use of a reflectance spectrophotometer as a quality control tool for herbal ingredients/products, specifically focusing on its ability to classify *C. xanthorriza* samples. A total of 65 pellets each for *C. xanthorriza* samples A and B were used as training data, with their reflectance spectra measured. The spectrum data was pre-processed using the 9-point Savitsky-Golay smoothing technique and cut in the curcuminoid absorption region (400-480 nm) for evaluation with PCA. A PLS-DA classification model was then created. The performance of the classification model was assessed using test data from 25 pellet spectra of each *C. xanthorriza* sample (A and B). The performance parameters determined were sensitivity and specificity.

PCA was used initially to evaluate the quality grouping of *C. xanthorriza* samples based on their spectrum data. **Figure 5a** displays the score plot of the first two principal components, which account for 94% of the total data variance. The score plot indicates that PC1, which accounts for 78% of the variance, is responsible for the clear separation between sample A and sample B. Samples with high curcuminoid content (A) are concentrated in the negative part of PC1, while sample B is more projected towards the positive part of PC1. This tendency for samples with higher curcuminoid content to be projected in the negative part of PC1 can also be observed from PCA analysis of the UV-Vis spectrum of *Curcuma longa* compared to other *Curcuma* species[42].

The same training data was then used to create a PLS-DA classification model. This classification model was built using a two-class input classification strategy that incorporates both the training and test data samples. In the model, the *C. xanthorriza* sample class A is marked with a predicted probability value of 1, while the *C. xanthorriza* class B is assigned a probability value of 0. The discrimination rule is based on comparing the predicted Y values (class) with a discrimination threshold set at 0.5. Additionally, the threshold value is set at ±1 (i.e., above 1.5 or below -0.5). Samples with predicted values outside these upper or lower limits cannot be discriminated as *C. xanthorriza* A or B [43]. **Figure 5b** shows the prediction vs. reference plot for *C. xanthorriza* sample classes A and B. The plot demonstrates that the model can classify all training samples according to their class probability values. The *C. xanthorriza* sample A is predicted to have a value in the range of 1, and the *C.*

xanthorriza sample B in the range of 0. The high quality of the model predictions is indicated by an R^2 value of 0.9124/0.9029 (calibration/cross-validation) and an RMSE of 0.1479 and 0.1580 (calibration/cross-validation). Both model parameters meet the criteria for a good multivariate model [39,40].

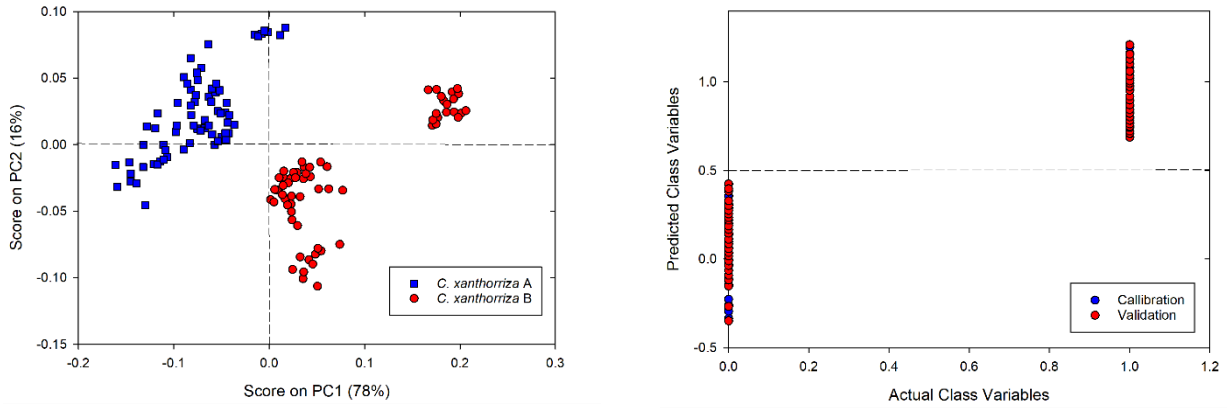

(a) (b)

Figure 5. (a) PCA score plot (PC1 and PC2) and (b) prediction performance of the PLS-DA classification model from training data on the spectrum of *C. xanthorriza* samples A and B.

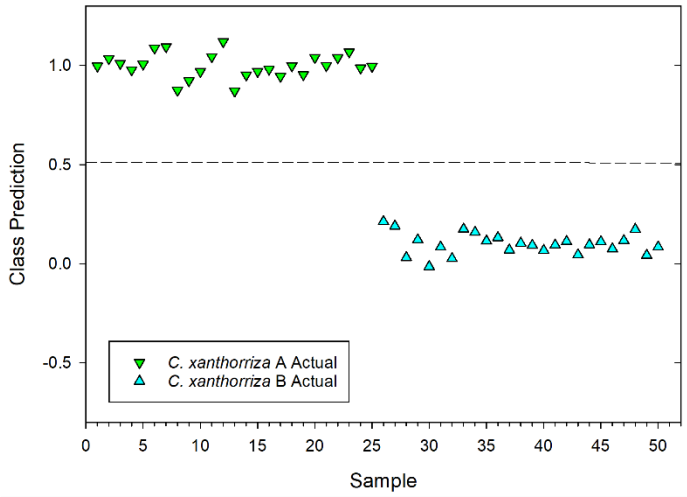

Figure 6. Binary classification plot for test data for *C. xanthorriza* samples A and B from the PLS-DA model.

The performance of the PLS-DA classification model was tested using test data that differed from the training data. The external validation data consisted of 25 pellets of *C. xanthorriza* sample A and 25 pellets of *C. xanthorriza* sample B. **Figure 6** displays a classification plot of the model prediction results for the two tested samples. The PLS-DA classification model correctly predicted the class of each sample. All sample A pellets had class probability values in the range of 1, and all sample B pellets had class probability values in the range of 0. This resulted in sensitivity and specificity values of 1, calculated using equations 3 and 4 with data from **Table 2**. Sensitivity and specificity values of 1 indicate that the model has an accuracy rate of 100% [24].

Further exploration of the performance of the reflectance spectrum-based classification model was carried out by determining the semi-quantitative parameters of the model, namely decision limit, detection capability, and unreliability region. The decision limit (CCα) is the minimum concentration of counterfeit (B) that the model will detect as positive when it is positive with probability p(x) = 5%. Below this limit, there is a 95% or higher probability of the model giving a negative prediction (meaning that sample A is pure or mixed with B to a lesser extent). Detection capability (CCβ) is the concentration of an adulterant in a sample that can be reliably detected and/or identified with statistical certainty p(x) = 95%. Above this limit, there is a 95% or higher probability that the model provides a positive output prediction for adulterated samples at adulterant concentrations above it. The unreliability region is the concentration range between the two limits where there is a certain probability (p(x) between 5% and 95%) of a negative error bias (FN) [44].

Table 2. Prediction confusion matrix for external validation data from the PLS-DA model.

		Actual Class	
		C. xanthorriza A	*C. xanthorriza* B
Predicted Class	*C. xanthorriza* A	TP = 25	FP = 0
	C. xanthorriza B	FN = 0	TN = 25

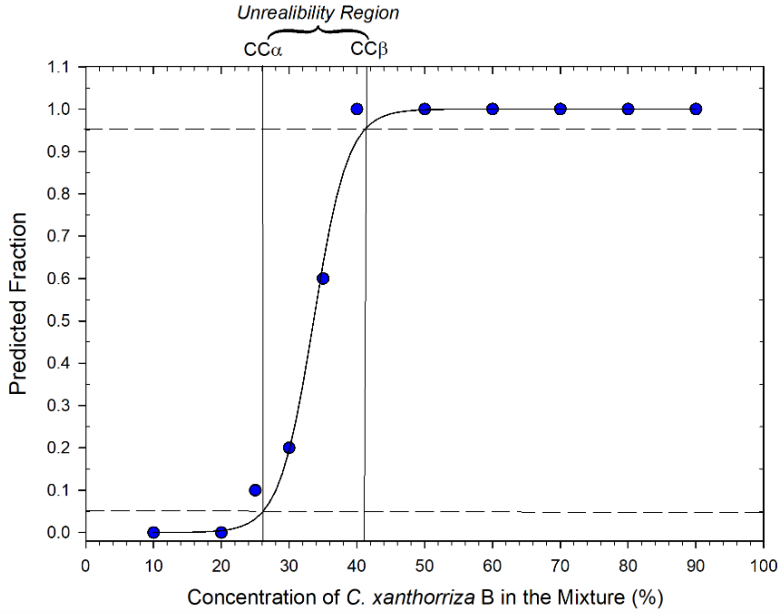

Figure 7. Performance characteristic curve (PCC) and semi-quantitative parameters from PLS-DA model prediction data. The sigmoid curve is generated from fitting the data to equation 5 with parameter values a = 33.60 and b = -0.3950.

Figure 7 displays the PCC curve and constraints of the semi-quantitative parameters of the model. The CCα value is obtained from the intersection of the PCC sigmoid curve with the horizontal black dotted line placed at p(x) = 0.05. CCβ is obtained from the intersection of the PCC sigmoid curve with the horizontal black dotted line placed at p(x) = 0.95. In this scenario, where *C. xanthorriza* sample A is adulterated by *C. xanthorriza* sample B, the PLS-DA classification model has a decision limit of 26.15% B, a detection capability of 41.06% B, and an unreliability region in the range of 26.15-41.06% B. The detection capability of the classification model from the reflectance spectrophotometer is still greater than the minimum limit for adulteration of herbal/spices raw materials considered economical in the market, such as saffron spices, which is 20% [45]. This is understandable because, in this case study, the adulterants are materials from the same species, differing only in terms of the content of the main components. In another case, the use of a fluorescence spectrometer combined with multi-way chemometrics resulted in a limit of quantification of different species adulterants for saffron of 24.3% [46].

4. CONCLUSIONS

The development of a visible light spectrophotometer using components from consumer electronics was carried out in this research. The spectrophotometer was built with reflectance measurement mode because this type allows for measuring samples, particularly herbal raw materials, in the solid state. The performance of the spectrophotometer was demonstrated by evaluating the entire spectrum data using chemometric methods. Two types of samples were used in this performance test: Sudan III and raw materials of *C. xanthorriza*. The reflectance spectrophotometer produced spectra of both samples, each with its own unique absorption characteristics. Principal component analysis (PCA) was able to group Sudan III standard samples based on their concentration and *C. xanthorriza* samples based on their curcuminoid content class. This indicates that the spectrum signal produced by the reflectance spectrophotometer can accurately represent the analyte content in the sample. Quantitative analysis of Sudan III levels in samples using the PLS regression model on reflectance spectrum data gave results that were comparable to those obtained using a commercial spectrophotometer. The PLS-DA classification model built from the spectrum of *C. xanthorriza* samples successfully discriminated between classes of *C. xanthorriza* with high accuracy. The classification model exhibited perfect sensitivity and specificity values and detection capabilities within acceptable limits. Based on the results of this research,

the reflectance spectrophotometer has the potential to be used as an alternative instrument for quality control of raw materials and herbal products.

ACKNOWLEDGMENTS

This work is part of a research project Contract No. 1655/IT3.11/PN/2018, supported by the Ministry of of Research, Technology and Higher Education, Indonesia, and the IPB University Indonesia.

REFERENCES

1. Badan Pengawas Obat dan Makanan. *Informatorium Obat Modern Asli Indonesia (OMAI) Di Masa Pandemi Covid-19 | Badan Pengawas Obat Dan Makanan*.; 2020. https://perpustakaan.pom.go.id/detail_buku_online/28676. Accessed July 15, 2024.
2. Torri MC. Innovative farmer institutions and market imperfections: New opportunities and challenges for the ayurvedic sector and small-scale enterprises in India. *J Entrep*. 2012;21(1):59-90. doi:10.1177/097135571102100103
3. Klein-Junior LC, De Souza MR, Viaene J, et al. Quality Control of Herbal Medicines: From Traditional Techniques to State-of-the-art Approaches. *Planta Med*. 2021;87(12-13):964-988. doi:10.1055/a-1529-8339
4. Ahmad Dar A, Sangwan PL, Kumar A. Chromatography: An important tool for drug discovery. *J Sep Sci*. 2020;43(1):105-119. doi:10.1002/jssc.201900656
5. Mao J, Xu J. Discrimination of herbal medicines by molecular spectroscopy and chemical pattern recognition. *Spectrochim Acta - Part A Mol Biomol Spectrosc*. 2006;65(2):497-500. doi:10.1016/j.saa.2005.11.030
6. Singh SK, Jha SK, Chaudhary A, Yadava RDS, Rai SB. Quality control of herbal medicines by using spectroscopic techniques and multivariate statistical analysis. *Pharm Biol*. 2010;48(2):134-141. doi:10.3109/13880200903059388
7. Stuth J, Jama A, Tolleson D. Direct and indirect means of predicting forage quality through near infrared reflectance spectroscopy. *F Crop Res*. 2003;84(1-2):45-56. doi:10.1016/S0378-4290(03)00140-0
8. Li M, Zhou X, Zhao Y, Wang DP, Hu XN. Quality assessment of Curcuma longa L. by gas chromatography-mass spectrometry fingerprint, Principle Components Analysis and Hierarchical Clustering Analysis. *Bull Korean Chem Soc*. 2009;30(10):2287-2293. doi:10.5012/bkcs.2009.30.10.2287
9. Lucio-Gutiérrez JR, Coello J, Maspoch S. Application of near infrared spectral fingerprinting and pattern recognition techniques for fast identification of Eleutherococcus senticosus. *Food Res Int*. 2011;44(2):557-565. doi:10.1016/j.foodres.2010.11.037
10. Rafi M, Nurcahyo B, Wahyuni WT, et al. Feasibility of UV-Vis Spectral Fingerprinting Combined with Chemometrics for Rapid Detection of Phyllanthus niruri Adulteration with Leucaena leucocephala. *Sains Malaysiana*. 2021;50(4):997-1006. doi:10.17576/jsm-2021-5004-10
11. Leary PE, Crocombe RA, Kammrath BW. Introduction to Portable Spectroscopy. *Portable Spectrosc Spectrom*. April 2021:1-13. doi:10.1002/9781119636489.ch1
12. Tubino M, Bianchessi LF, Vila MMDC. Quantitative spot-test analysis of metformin in pharmaceutical preparations using ultraviolet-visible diffuse reflectance spectroscopy. *Anal Sci*. 2010;26(1):121-124. doi:10.2116/analsci.26.121
13. Scheeline A. Spectrometry with consumer-quality CMOS cameras. *Mob Heal Technol Methods Protoc*. 2015;1256:259-275. doi:10.1007/978-1-4939-2172-0_18
14. Silva WRF, Suarez WT, Reis C, et al. Multifunctional Webcam Spectrophotometer for Performing Analytical Determination and Measurements of Emission, Absorption, and Fluorescence Spectra. *J Chem Educ*. 2021;98(4):1442-1447. doi:10.1021/acs.jchemed.0c01085
15. Abbasi H, Nazeri M, Mireei SA. Design and development of a LabVIEW-based LED-induced fluorescence spectroscopy system with applications in non-destructive quality assessment of agricultural products. *J Phys Conf Ser*. 2016;672(1):012010. doi:10.1088/1742-6596/672/1/012010
16. Liang Y-Z, Xie P-S, Chan K. Chromatographic Fingerprinting and Metabolomics for Quality Control of TCM. *Comb Chem High Throughput Screen*. 2010;13(10):943-953. doi:10.2174/138620710793360310
17. Sima IA, Andrási M, Sârbu C. Chemometric assessment of chromatographic methods for herbal medicines authentication and fingerprinting. *J Chromatogr Sci*. 2018;56(1):49-55. doi:10.1093/chromsci/bmx080
18. Bian X, Lu Z, Van Kollenburg G. Ultraviolet-visible diffuse reflectance spectroscopy combined with chemometrics for rapid discrimination of Angelicae Sinensis Radix from its four similar herbs. *Anal Methods*. 2020;12(27):3499-3507. doi:10.1039/d0ay00285b
19. Bian XH, Zhang RL, Wang J, Liu P, Lin LG, Tan XY. Rapid quantification of adulterated Panax notoginseng powder by ultraviolet-visible diffuse reflectance spectroscopy combined with chemometrics. *Chinese J Anal Chem*. 2022;50(3):100055. doi:10.1016/j.cjac.2022.100055
20. Das A. Portable UV–Visible Spectroscopy – Instrumentation, Technology, and Applications . *Portable Spectrosc Spectrom*. April 2021:179-207. doi:10.1002/9781119636489.ch8
21. Scheeline A. Smartphone Technology – Instrumentation and Applications. *Portable Spectrosc Spectrom*. April 2021:209-235.

doi:10.1002/9781119636489.ch9
22. Rahmat E, Lee J, Kang Y. Javanese Turmeric (Curcuma xanthorrhiza Roxb.): Ethnobotany, Phytochemistry, Biotechnology, and Pharmacological Activities. *Evidence-Based Complement Altern Med*. 2021;2021(1):9960813. doi:10.1155/2021/9960813
23. Simamora A, Timotius KH, Yerer MB, Setiawan H, Mun'im A. Xanthorrhizol, a potential anticancer agent, from Curcuma xanthorrhiza Roxb. *Phytomedicine*. 2022;105:154359. doi:10.1016/J.PHYMED.2022.154359
24. Cuadros-Rodríguez L, Pérez-Castaño E, Ruiz-Samblás C. Quality performance metrics in multivariate classification methods for qualitative analysis. *TrAC - Trends Anal Chem*. 2016;80:612-624. doi:10.1016/j.trac.2016.04.021
25. López MI, Callao MP, Ruisánchez I. A tutorial on the validation of qualitative methods: From the univariate to the multivariate approach. *Anal Chim Acta*. 2015;891:62-72. doi:10.1016/j.aca.2015.06.032
26. Poh AH, Jamaludin MF, Fadzallah IA, et al. Diffuse reflectance spectroscopic analysis of barium sulfate as a reflection standard within 173–2500 nm: From pure to sintered form. *J Near Infrared Spectrosc*. 2019;27(6):393-401. doi:10.1177/0967033519868241
27. Balado Sánchez C, Díaz Redondo RP, Fernández Vilas A, Sánchez Bermúdez AM. Spectrophotometers for labs: A cost-efficient solution based on smartphones. *Comput Appl Eng Educ*. 2019;27(2):371-379. doi:10.1002/cae.22081
28. Amma SI, Luo J, Pantano CG, Kim SH. Specular reflectance (SR) and attenuated total reflectance (ATR) infrared (IR) spectroscopy of transparent flat glass surfaces: A case study for soda lime float glass. *J Non Cryst Solids*. 2015;428:189-196. doi:10.1016/j.jnoncrysol.2015.08.015
29. Small GW. Chemometrics and near-infrared spectroscopy: Avoiding the pitfalls. *TrAC - Trends Anal Chem*. 2006;25(11):1057-1066. doi:10.1016/j.trac.2006.09.004
30. López MI, Colomer N, Ruisánchez I, Callao MP. Validation of multivariate screening methodology. Case study: Detection of food fraud. *Anal Chim Acta*. 2014;827:28-33. doi:10.1016/j.aca.2014.04.019
31. Yang SK, Zhang JP, Xu YH, Deng XN. Ultraviolet-visible absorption spectral properties of sudan III in different solvents. *Guang Pu Xue Yu Guang Pu Fen Xi/Spectroscopy Spectr Anal*. 2007;27(2):325-328. https://pubmed.ncbi.nlm.nih.gov/17514967/. Accessed July 16, 2024.
32. Taunaumang H, Tuladi D, Wakary P. Physical Structure Analysis and Optical Properties of Sudan III Thin Film. *Adv Mater Phys Chem*. 2021;11(06):101-110. doi:10.4236/ampc.2021.116010
33. Pastres R, Panzeri AL, Visentin D, Causin V. Determination by infrared spectroscopy of triacetin content in diesel: A tool for countering designer fuel frauds. *Talanta Open*. 2022;5:100109. doi:10.1016/j.talo.2022.100109
34. Suresh H, Behera AR, Selvaraja SK, Pratap R. Quantification of Curcuminoids in Turmeric Using Visible Reflectance Spectra and a Decision-Tree Based Chemometric Approach. *J Electrochem Soc*. 2020;167(16):167528. doi:10.1149/1945-7111/abd603
35. Kim HJ, Kim DJ, Karthick SN, et al. Curcumin dye extracted from Curcuma longa L. used as sensitizers for efficient dye-sensitized solar cells. *Int J Electrochem Sci*. 2013;8(6):8320-8328. doi:10.1016/s1452-3981(23)12891-4
36. de Araújo Gomes A, Azcarate SM, Špánik I, Khvalbota L, Goicoechea HC. Pattern recognition techniques in food quality and authenticity: A guide on how to process multivariate data in food analysis. *TrAC - Trends Anal Chem*. 2023;164:117105. doi:10.1016/j.trac.2023.117105
37. Heryanto R, Iswantini D, Rohaeti E, Rafi M, Mulyati, Pamungkas WS. the Development and Quantitative Performance Test of Low-Cost Visible Spectrophotometer and Its Comparison With Commercial Spectrophotometer. *Malaysian J Anal Sci*. 2023;27(3):463-470. https://www.scopus.com/inward/record.uri?eid=2-s2.0-85164156272&partnerID=40&md5=1bc05980222fccb0dfe76a01a13d2a34.
38. Alomar TS, AlMasoud N, Xu Y, et al. Simultaneous Multiplexed Quantification of Banned Sudan Dyes Using Surface Enhanced Raman Scattering and Chemometrics. *Sensors*. 2022;22(20):7832. doi:10.3390/s22207832
39. Williams P, Antoniszyn J. *Near-Infrared Technology: Getting the Best out of Light*. First edit. [Stellenbosch, South Africa]: African Sun Media under the Sun Press imprint; 2019. doi:10.18820/9781928480310
40. Wu X, Li G, Fu X, He F, Wu W. Effect of spectrum measurement position on detection of Klason lignin content of snow pears by a portable NIR spectrometer. *Food Energy Secur*. 2023;12(3):e447. doi:10.1002/fes3.447
41. Heil K, Schmidhalter U. An evaluation of different nir-spectral pre-treatments to derive the soil parameters c and n of a humus-clay-rich soil. *Sensors*. 2021;21(4):1-24. doi:10.3390/s21041423
42. Rafi M, Jannah R, Heryanto R, Kautsar A, Septaningsih DA. UV-Vis spectroscopy and chemometrics as a tool for identification and discrimination of four Curcuma species. *Int Food Res J*. 2018;25(2):643-648.
43. Jiménez-Carvelo AM, Arroyo-Cerezo A, Bikrani S, Jia W, Koidis A, Cuadros-Rodríguez L. Rapid and non-destructive spatially offset Raman spectroscopic analysis of packaged margarines and fat-spread products. *Microchem J*. 2022;178:107378. doi:10.1016/j.microc.2022.107378
44. Ruisánchez I, Rovira G, Callao MP. Multivariate qualitative methodology for semi-quantitative

information. A case study: Adulteration of olive oil with sunflower oil. *Anal Chim Acta*. 2022;1206:339785. doi:10.1016/j.aca.2022.339785

45. Petrakis EA, Cagliani LR, Polissiou MG, Consonni R. Evaluation of saffron (Crocus sativus L.) adulteration with plant adulterants by1H NMR metabolite fingerprinting. *Food Chem*. 2015;173:890-896. doi:10.1016/j.foodchem.2014.10.107

46. Chen Y, Wu HL, Wang T, et al. Rapid detection and quantification of adulteration in saffron by excitation–emission matrix fluorescence combined with multi-way chemometrics. *J Sci Food Agric*. 2024;104(3):1391-1398. doi:10.1002/jsfa.13028